

Impact of open de-ionized water thin film laminar immersion on the liquid immersed ablation threshold and ablation rate of features machined by KrF excimer laser ablation of bisphenol A polycarbonate.

C.F. Dowding and J. Lawrence

Wolfson School of Mechanical and Manufacturing Engineering, Loughborough University,
Leicestershire, LE11 3TU, UK.

Correspondence

Mr. Colin Dowding

Wolfson School of Mechanical and Manufacturing Engineering,
Loughborough University,
Leicestershire,
LE11 3TU,
Great Britain.

Tel : +44 (0)1509 227593

Fax : +44 (0)1509 227648

e-mail : c.f.dowding@lboro.ac.uk

Abstract

Debris control and surface quality are potential major benefits of sample liquid immersion when laser micromachining; however, the use of an immersion technique potentially modifies the ablation mechanism when compared to an ambient air interaction. To investigate the machining characteristics, bisphenol A polycarbonate has been laser machined in air and under a controllable open liquid film. To provide quantitative analysis, ablation threshold, ablation rate and the attenuation coefficient of the immersing DI water fluid were measured. In ambient air the threshold fluence was measured to be 37 mJ.cm^{-2} . Thin film immersion displayed two trends: threshold fluences of 58.6 mJcm^{-2} and 83.9 mJcm^{-2} . The attenuation of DI water was found to be negligible; thus, the change in ablation rate resulted from increased confinement of the vapour plume by the liquid medium, generating higher *Bremsstrahlung* attenuation of the beam, lowering the laser etch rate. Simultaneously, splashing motivated by the confined ablation plume allowed release of plume pressure before plume etching commenced. This contributed to the loss of total etching efficiency. Two interaction scenarios were observed as a result of splashing: (i) intermediate threshold fluence, where splashing occurred after every pulse in a mode that interrupted the flow entirely, leaving an ambient air interaction for the following pulse; (ii) high threshold fluence, where splashing occurred for every pulse in a mode that allowed the flow to recommence over the image before the next pulse causing every pulse to experience *Bremsstrahlung* attenuation. Since attenuation of the immersion liquid was negligible, it is the action of the constrained ablation plume within a thin flowing immersion liquid, the resultant *Bremsstrahlung* attenuation and splashing events that are the critical mechanisms that modify the primary ablation characteristics.

Introduction

The use of liquid immersion ablation was attempted primarily with the intention of debris control during excimer laser micromachining of Bisphenol A polycarbonate, alternatively known as lexan [1]; however, Dowding [2] found that the use of thin film laminar flow water immersion during excimer ablation of bisphenol A polycarbonate resulted in a reduction in surface roughness of machined features. This effect has potential benefits for micro lens array manufacture where profile accuracy is key [3]. The reduction in surface roughness is an interesting phenomenon with many possible causes. The smoothing effect of liquid immersion observed by Dowding [2] suggests the ablation mechanism is altered significantly by the action of laminar flow liquid immersion. This may result in an alteration to two primary parameters used for measuring pulsed laser machining efficiency: (i) the ablation threshold; (ii) the ablation rate.

Up to this time all research into liquid immersion assisted laser machining has involved stagnant liquid. This work explores for the first time the impact of laminar flow liquid immersion on ablation rate and ablation threshold, using the data gleaned to identify any differences in the machining mechanism between ablation in ambient air and under laminar flow liquid immersion.

All mediums through which electromagnetic radiation passes present resistance to progress dependent upon medium characteristics and wavelength [7]. The use of a liquid to cover a material to be ablated poses an added complexity to the beam path. The light must pass from the demagnifying optic, into ambient air, then into de ionized (DI) water before colliding with a sample surface, whereafter the beam should reach focus. At every medium interface the beam will encounter changes in refractive index, modifying the focal length of the demagnified beam. Each new medium poses losses to beam energy through reflectance and attenuation [6,7]. This loss of beam energy will result in lower beam fluence at the image. Lower fluence should correspond with a lower ablation rate [8]; therefore it is expected that the depth of a feature machined under liquid immersion will be lower than that of a corresponding feature machined in ambient air.

The ablation rate and threshold are dependent upon the ablation mechanism that removed the material to produce the feature. This ablation mechanism is a complex and contentious subject, with recent literature alluding to a number of mechanisms that work together simultaneously [11-**Error! Reference source not found.**]. The most common practice for laser micromachining is for ablation to take place in an ambient air environment, allowing simple material loading and rapid processing times without the need for time consuming gas evacuation procedures. The ablation mechanism is also material specific, with much debate surrounding the exact nature of polymer interactions with short wavelength laser beams. In the case of a 248 nm beam interacting with a polymer material in ambient air, the theory of explosive evaporation, postulated by Kelly and Miotello [17], which accounts for a primarily photochemical interaction with a photothermal element active between beam photons and the material's atomic matrix. Yang [19] develops on this to explain that formation of ablation products during pulsed laser ablation, PLA, in gasses is a result of condensation of the plasma plume generated by the ejection of ablated gaseous products from the solid target. In this scenario, there are three critical stages, generation, transformation and condensation. The key stage with respect to a machined feature is the generation phase. In the case of laser ablation in a gas at atmospheric pressure, the vapour plume can expand relatively unimpeded as there is little difference in density and viscosity between the vapour plume and surrounding atmosphere as described in Figure 2. When ablating material beneath a film of liquid the interaction between beam, plume and material changes: the expansion of the plume is now restricted by the increased viscosity of the surrounding liquid [20]; molecules attempting to escape the plume are prevented by the plume/liquid interface as described in Figure 2. The confinement of the ablation plume has been found by Zhu *et al.* [**Error! Reference source not found.**] to etch the surface of the workpiece. Zhu *et al.* claim the optimum film thickness for ablation rate to be approximately 1.1mm. Recently Elaboudi *et al.* [**Error! Reference source not found.**-**Error! Reference source not found.**] have conducted experiments using 248 nm excimer pulsed radiation to ablate polymer targets including polycarbonate. These results provide support for the findings of previous authors: the ablation threshold decreases when using liquid immersion (Elaboudi *et al.* use ultrapure water) compared to traditional ablation in ambient air; photomechanical interactions driven by thermal evaporation are primarily responsible for the ejection of debris

material; typically debris generated had a diameter of 50 nm and a chemistry close to that of the original material, supporting a “cold” or photomechanical removal mechanism. Another theory postulated by these authors [**Error! Reference source not found.**] is that some debris is generated by a hydrolysis reaction for immersed PET ablation in addition to photochemical degradation as an explanation for the decreased ablation threshold of the PET when immersed in ultra pure water. The use of excimer laser radiation also has been shown to have an impact on the morphology and microstructure of polycarbonate. Parvin *et al.* [26] use 248 nm excimer radiation amongst other wavelengths to irradiate polycarbonate samples. Use of high fluences (6 J.cm^{-2}) resulted in extensive crosslinking of the polycarbonate microstructure, thus generating significant surface hardening of the material. Zangeneh *et al.* [27] credit this increase in surface hardness to a change in the size and population of the micro cone shaped microstructure of the material, which increase drastically at high laser fluences.

MAIN TEXT

Experimental Procedures

Materials

Bisphenol A polycarbonate (Holbourne Plastics, Ltd), was as received in 1200 mm x 1000 mm sheets of 0.5 mm thickness. Prior to excimer laser processing, the bisphenol A polycarbonate sheet was cut into rectangular sections of 30 mm x 10 mm using scissors, as this is a shear cutting technique which avoids production of debris. Protective cover sheets were then peeled off each sample.

Laser Processing Procedure

An excimer laser (EMG 203 MSC; Lambda Physique, GmbH) using KrF as the excitation medium was used to produce a pulsed beam with a wavelength of 248 nm and pulse duration of 25 ns. Thereafter the beam was supplied to a laser micromachining optics assembly (EX-PS-500; Exitech Ltd), where the raw beam was homogenised in the x- and y-axis before being passed through a stainless steel mask to produce either a square or circular objective beam. The masked beam was then

demagnified by 15x to produce an ablation spot with a depth of focus (DoF) of 6 μm . A profile of the masked beam has been obtained using a beam profiler (SP620U; Spiricon, Ltd). As one can see from Figure 3, it demonstrates a lack of squareness to the beam profile. In this instance this causes greater power density on the left of the mask.

Immersing any sample to be machined under a thin film laminar flow of DI water presents significant technical challenges. The possibility of beam generated splashing means an enclosure to the test rig is required to protect the tool optics from water damage whilst maintaining a stable environment within which to machine. In this work a fused silica window was used to allow the beam to pass into the enclosure with minimum loss as shown schematically in Figure 4. However, the masked and demagnified beam was not collimated on the tool used; thus when it passed through the fused silica window of the enclosure the focal length of the beam was modified. The tool used for these experiments used an auto focussing system. This meant the correct focal length of the tool without the enclosure, to which the sample is set before the experiment was conducted, would be outside the focal range of the tool when the enclosure window was installed. This is the reason for the poor focus experienced by Dowding [2]. To check the effect of focus modification using liquid immersion, accurate dry focus must be maintained; hence the window had to be removed. Even without the enclosure window the use of an immersion liquid presented complexities for the beam path.

As shown in figure 4 the sample was mounted on a stainless steel table by means of the capillary action of isopropyl alcohol (IPA) which was applied to the sample table before the sample was mounted. The table was located to a pivot cradle by a tongue and groove arrangement twined with a dowel for linear constraint - magnets allowed simple and secure repeatable fixing between the table and cradle. The cradle allowed the table to be tilted around its mid-point by use of an adjustable thumb screw that supported the water inlet end of the table. This tilt mechanism had two experimental applications. First it allowed the angle of incidence between the excimer laser beam and the sample to be modified. Second, it allowed the run-off rate of the liquid to be changed independently of the supplied liquid flow rate; hence the film thickness on the sample could be controlled. Liquid was supplied by use of gravity feed from a butt supported at a constant height. The supply was gated by a

valve to allow rudimentary control of flow rate before being delivered through a flat nozzle mounted 0.5 mm above the sample. The sample table and water nozzle were positioned over a miniature basin with a hose leading to a sealed storage tub positioned a distance below the basin, again using gravity feed to ensure evacuation of liquid from the basin.

The basin geometry also provided location for a clear perspex enclosure within which a controlled environment for experiments could be maintained. That enclosure provided repeatable location for the water nozzle with respect to the basin and therefore sample table. The enclosure was not entirely sealed for the purpose of maintaining more accurate focus for these experiments, as described above. This did present a danger to the tool optics from beam-generated splashing of the immersion liquid; but with the use of a small orifice this possibility was minimized.

During normal open use the rig was mounted on a driven lift stage that was adapted to dynamically adjust the sample height dependent upon a signal generated by logical interpretation of the deflection of a reflected reference beam. With the inclusion of the perspex enclosure for these experiments; however, the reference beam was obstructed and this dynamic focussing method could not be used. Instead the sample height is set before the experiment to being as close to the centre of DoF as possible, then the stage is set to maintain its location whilst the sample and enclosure are mounted to it, as the dry samples displayed in figure 5 show, this is a viable method for finding focus with this equipment. The depth of focus, DoF, also played an important role in limiting the tilt angle (for a 500 μm diameter spot size the maximum tilt angle possible whilst keeping the entire image inside focal tolerance is 1.36° , assuming the centre of the image lies at the pivot axis)

Each sample was used for only one test to prevent cross-contamination. After lasing ended the enclosure was removed and the sample placed into a cell of a sealed sample tray to protect it from atmospheric dust.

Samples were produced separately for ambient air and liquid immersion. To measure ablation threshold separate samples were produced whilst requesting the laser pulse energies listed in column A of Table 1. These requested pulse energies delivered the spot energies listed for ambient air and

liquid immersion in columns b and c respectively of Table 1. All beam energy values quoted in this work were measured using a power meter head (LMP 10i, Coherent, Inc) connected to a reader unit (Labmaster; Coherent, Inc). Spot energies were measured twice for each sample - once before the sample was machined and once after the sample was machined. In this way any change in the beam between measurements was accounted for. The image spot diameter for the dry samples was 650 μm ; the spot diameter used for the liquid immersion was 530 μm . To measure the ablation threshold in ambient air 500 pulses were used at 10 Hz, measured by opening the laser shutter for 50 s. Assuming a human accuracy of ± 0.15 s, a pulse number error of ± 1.5 can be quoted for these results. To measure the ablation threshold for liquid immersion 150 pulses were used at a rate of 30 Hz, measured by opening the shutter for 5 s. Assuming the same human accuracy as that estimated for the ambient air samples gives a pulse number error of ± 4.5 . The lower number of pulses used for the immersion samples was a requirement because the DI water supply was limited to a small butt and the extraction system became overwhelmed quickly by water volume as it did not include an extraction pump.

To produce ablation rate samples a laser pulse energy of 200 mJ was requested for all samples. Again the spot energy for every sample was measured both before and after the sample was machined, with the average of these two values stated for the corresponding sample in columns B and D of Table 2. Samples were produced using differing numbers of pulses. These numbers are displayed in columns A and C of Table 2.

Sample Analysis Techniques

Because depth measurement using an optical microscope requires human judgement, the ablation depths were measured using a dragged needle profiler (CM300 Talysurf; Taylor-Hobson, Ltd). As such, any possibility of profile error was minimized.

Results and Discussion

Effects of thin film laminar flow water immersion ablation on Ablation Threshold

The ablation threshold can offer insight into the nature of the ablation mechanism at work in a beam – material interaction. In the case considered herein the beam and material remain the same, but the mechanics of that interaction in terms of chemical reactions, *Bremsstrahlung* attenuation of the plume and the contribution of plume etching to the removal of material yield a significant modification to the ablation threshold. Two data sets (ablation in ambient air and ablation under thin film laminar flow DI water immersion) are plotted in graph Figure 6. The plot of data for the sample machined in ambient air shows a strong linear correlation, with all the results being tightly packed around the trend line. This would suggest that the threshold value yielded for ablation in ambient air is accurate. The data plotted for immersion machined samples includes four anomalies, plotted as triangles in Figure 6. This is interesting as these four anomalies appear to lie in a trend, which yields an intermediate threshold fluence value between ablation in ambient air and under typical liquid immersion. The intermediate group could be caused by either one of three occurrences or a combination thereof: (i) The liquid flow changes in geometry with respect to time due to natural turbulence generated surface ripple; thus a thinner or non-existent liquid coating to the material surface may have been present for a period during the machining of anomalous results. (ii) Ablation plume generated splashing could also cause significant geometric change to the liquid flow with a similar result: the plume, which becomes compressed by the high viscosity of the immersion liquid to a pressure that is uncontainable by a thin film of covering fluid, results in liquid rupture and splashing. The result of such splashing is an uncovered section of the sample in the flow, thus allowing a following pulse unobstructed access for ablation in an ambient air interaction, surrounded by flowing liquid. This is inline with the findings of Zhu et al. [**Error! Reference source not found.**] (iii) The focus of the anomalous results could have been unusually good when compared to the general trend of these samples as all the anomalous results were greater than the trend. This is a situation that is a consequence of changing immersion fluid surface geometry, where non-repeatable flow geometry could act to focus or defocus the beam with respect to time, resulting in varying fluence levels, and varying etch depths. This effect would result in a widened spectrum of depth data, rather than the clear data groupings demonstrated in this data.

The threshold fluence for bisphenol A polycarbonate is only 37.7 mJcm^{-2} in ambient air, indicating the excellent machining attributes that bisphenol A polycarbonate poses for excimer laser machining. Such a finding is in accord with those of Lemoine *et al.* [10]. In contrast, the non-anomalous plot for thin film laminar flow water immersion machined samples require 66.7 mJcm^{-2} , a significant increase in threshold fluence over the sample machined in ambient air. This goes against the findings of Fabbro *et. al* [20] and Elaboudi *et al.* [**Error! Reference source not found.-Error! Reference source not found.**], who found that the use of liquid immersion using thicker, stagnant films of ultrapure water greatly reduced the ablation threshold. According to Zhu *et al.* an optimum flow thickness for liquid immersion ablation exists [**Error! Reference source not found.**], occurring at around 1.1mm. Since film thickness is critical, then it is reasonable to postulate that the beam passes through the medium to the sample as normal and ablation commences, generating an ablation plume; the liquid restricts the expansion of the plume, compressing it, increasing its optical density with respect to a similar plume unimpeded in ambient air, thus resulting in greater *Bremsstrahlung* attenuation and lower laser etch rates. Simultaneously, the increased pressure of the plume, in union with the thin (less than 1.1mm thickness) laminar film causes rupture of the flow, resulting in splashing of the immersion liquid and a loss of plume pressure before the plume etch threshold of the material is achieved. Hence the laser etch rate is decreased without the addition of plume etching that normally occurs when using thick (over 1.1mm) films. This indicates that the four erroneous data points plotted in Figure 6 were machined in a situation where the etching contribution given by the laser beam was higher: The splashing occurred in a mode that allowed more pulses to arrive at the sample surface without having to pass through a liquid medium, thus not experiencing the *Bremsstrahlung* attenuation of the compressed plume generated by the previous pulse, giving a lower effective threshold fluence at the image.

The gradients shown in Figure 6 for ambient air and thin film laminar flow water immersion machining suggest that the ablation rate response of liquid immersion with increasing fluence is greater than the response of ablation in ambient air. Further inspection of the plot gradients yields support for the explanation of the anomalous results detailed above. The anomalous data points

display the steepest gradient and all fall close to the trend line. This observation supports the idea that changes in liquid flow geometry gives increased ablation rate rather than the effects of randomly improved focus. The precise cause of this change in geometry can also be attributed using the gradient as evidence; for if the erroneous results were purely due to nozzle generated flow variations the gradient would have been similar to that of the non-anomalous results, but less tightly packed around the trend line as this would be a random error response. More likely is a change in liquid geometry due to plume generated splashing: as fluence rises, volumes of water removed from the flow by splashing are proportionate. Consequently higher fluence pulses result in greater exposure of the surface to ambient air and more exposure to an ambient air level of laser etching [2].

Effects of thin film laminar flow water immersion ablation on Ablation Rate

The ablation rates for bisphenol A polycarbonate machined in ambient air and under thin film laminar flow water immersion are shown in Figure 7. The ablation rate gives useful information concerning volumetric removal of material once above the fluence threshold of the material and will give further insight into efficiency of etching under a thin laminar flow water film. It must be noted that the plot made in ambient air is less prone to error due to the higher number of pulses used. Despite the small number of pulses used to collate data for immersion ablation, the plot generated shows that every point is close to the trend line; thus an accurate measurement of the true ablation rate has been obtained.

Figure 7 demonstrates laser machining in ambient air offers higher ablation rates than thin film laminar flow water immersion machining as would be expected given the threshold fluence values determined from Figure 6, but the decrease in ablation rate due to the use of immersion ablation is not significant. The difference between the gradients of the trend lines for ablation in ambient air and under thin film laminar flow water immersion is 0.09, showing a drop in ablation rate of 20%. It was expected that ablation rate in liquid would be lower than that of ambient air; if the threshold fluence for removal of material in ambient air is half that required under liquid immersion, it can be expected that removal of material will continue at a similarly high rate once the fluence threshold is exceeded. Instead the difference in ablation rate is minimal (50% was expected, 20% measured), once again

supporting the proposed scenario stated above, where ablation plume motivated splashing of the immersion fluid film releases the plume vapour and allows less *Bremsstrahlung* attenuation of the following pulse.

De Ionized Water Attenuation of excimer laser radiation.

The results of the ablation threshold and rate experiments detailed above are interesting; they raise two potential reasons for the response to medium change: (i) increased *Bremsstrahlung* attenuation generated by restricted plume expansion as described by Zhu *et al.* [**Error! Reference source not found.**], without the plume etching mechanism that normally accompanies plume compression due to vapour plume motivated splashing of the immersion film before plume the plume etch pressure threshold of the sample is achieved; (ii) the attenuation of the DI water medium is significantly different to that of air and is attenuating the beam on route to the sample and lowering the image fluence. For conclusive support for one of these possibilities the attenuation of the immersion medium was measured. A special pot has been manufactured, using a fused silica slide that has been epoxy resin bonded to a transparent acrylic tube which is internally marked with a millimetre scale. This pot was placed on top of the power meter head, both of which are a significant distance below the focal point of the optics. The mask used for this experiment would give a 500 μm diameter circular spot at focus. The water level and corresponding readings taken are plotted in Figure 8. The effect of increasing water depth for the beam to pass through is small. Most fluctuations in the values can be explained by the random variations in pulse energy, pulse to pulse, inherent of excimer lasers. Thus it follows that the loss of etch rate by use of liquid immersion must be a mechanism other than immersion medium attenuation of the laser beam. Hence this result gives further support for the proposal that splashing and the mode of splashing with regard to the loss of plume etching and increase in *Bremsstrahlung* attenuation is the reason for a loss in lasing efficiency. Indeed, the findings of Fabbro *et al.* [20] and Elaboudi *et al.* [**Error! Reference source not found.-Error! Reference source not found.**] showed for open thick film immersion lasing efficiency is increased, but Xhu *et al.* [**Error! Reference source not found.**] showed that the effectiveness of an open film is limited to a critical film thickness of 1.1mm. The findings in this work were obtained using a film

thickness much lower than 1.1mm. It must be noted that the fluence of the beam at the surface of the liquid is insufficient to cause splashing, thus the effect of splashing to the loss of beam energy cannot be measured with this technique. It would be of interest to define a magnitude for the effect of splashing by placing a pool of water in the DoF of the laser optics and taking a set of beam energy readings for differing energies and liquid depths. Nevertheless the findings herein are insightful insofar as they show that a loss in lasing fluence, and therefore efficiency, is not the result of the DI water liquid medium when using open thin film laminar flow immersion assisted machining, but is caused by the interaction between vapour plume, beam and surrounding thin liquid medium.

Conclusions

Measurements of ablation threshold and ablation rate when KrF excimer laser machining bisphenol A polycarbonate samples in ambient air and immersed in a thin film laminar flow of DI water showed differences in the machining mechanisms. In ambient air the threshold fluence was measured to be 37 mJcm^{-2} with an ablation rate of $0.459 \text{ }\mu\text{m/pulse}$, under thin film immersion two trends were identified, giving threshold fluences of 58.6 mJcm^{-2} and 83.9 mJcm^{-2} respectively, the ablation rate for immersed samples was measured to be $0.367 \text{ }\mu\text{m/pulse}$. The attenuation coefficient of the immersing DI water was measured separately and found to be negligible.

The observed change in ablation rate and ablation threshold cannot be directly explained by the attenuation coefficient of the water medium. It is believed that the change in ablation rate was generated by the increased confinement of the vapour plume by the liquid medium during immersion ablation. This in turn generated higher *Bremsstrahlung* attenuation of the beam and subsequently produced the observed 20% reduction in the laser etching rate from $0.459 \text{ }\mu\text{m/pulse}$ to $0.367 \text{ }\mu\text{m/pulse}$. This is reasonable because in contrast to thick film liquid immersion where the confinement and resultant increased pressure of the plume etches the sample to a greater extent than the laser, the ablation plume can only be constricted to a limited extent by thin film laminar flow immersion before the ablation plume causes rupture and splashing of the immersion liquid. This means that the beam

still experiences some extra *Bremsstrahlung* attenuation before liquid rupture occurs, but the action of plume etching is nonexistent for thin films.

The observed splashing of the thin film laminar flow DI water during excimer laser machining was recorded in the data spread. This suggests that two independent interaction types are active: (i) an intermediate threshold fluence level where splashing occurs after every pulse in a mode that interrupts the flow entirely. This leaves an ambient air interaction for the following pulse; (ii) a high threshold fluence level where splashing occurs for every pulse in a mode which allows the flow to recommence over the image before the next pulse. This results in every pulse experiencing high *Bremsstrahlung* attenuation. These two scenarios show a relationship between pulse fluence and fluid rupture timing, where medium fluence causes maximum flow disruption by splashing and high fluence results in instantaneous but short term interruption of the flow.

Further verification was obtained from measurement of the attenuation of the immersing liquid, which was found to be negligible. This establishes that the immersing liquid is not in itself responsible for the loss of fluence at the image and therefore lasing efficiency, but instead is the consequence of the action of the ablation plume when constrained within a thin flowing immersing liquid and the resultant *Bremsstrahlung* attenuation and splashing events that occur. Clearly it is the interaction of the confined plume with the beam, combined with the inability of the plume to etch the surface of the sample that is of importance.

References

- 1 Dowding, C. F. and Lawrence, J. "Use of thin laminar liquid flows above ablation area for control of ejected material during excimer machining", The proceedings of The 27th International Congress on Application of Lasers and Electro-Optics: Laser Materials Processing Section, 2008, pp.872-880.
- 2 Dowding, C. F., and Lawrence, J. "Use of thin laminar liquid flows above ablation area for control of ejected material during excimer machining", IMECHE Proceedings B, 2009, 223, 6, pp.
- 3 Gower, M. C. "Excimer laser microfabrication and micromachining", Laser Precision Microfabrication, RIKEN Review, 2001, pp.50-56.
- 4 Kim, J. Y., Sohn, D., Kim, E. R. "Polymer-based multi-layer conductive electrode film for plastic LCD applications", Applied Physics A, 2001, **72**, 6, pp.699-704.
- 5 Rizvi, N. H., Rhumsby, P. T., and Gower, M. C. "New Developments and Applications in the Production of 3D Micro-structures by Laser Micro-machining", Proceedings of SPIE, 1999, **3898**, 240.
- 6 Hecht, E. "Optics", 1998, **3**. Addison Wesley Longman, New York.
- 7 Gray, D. E. "American Institute of Physics Handbook", 1972, **3**. McGraw-Hill, London.
- 8 Loudon, R. "The Quantum Theory of Light", 2000, **4**, Oxford University Press.
- 9 Dyer, P. E. "Excimer laser polymer ablation: twenty years on", Applied Physics A, 2003, 77, pp.167-173.
- 10 Lemoine, P., Magan, J.D., Blau, W.J. "Photoablative etching of materials for optoelectronic integrated devices" Proceedings of SPIE, 1991, **1377**, 45, pp.45-56.
- 11 Yung, K. C., Mei, S. M., and Yue, T. M. "Pulsed UV laser ablation of a liquid crystal polymer", International Journal Of Advanced Manufacturing Technology, 2005, 26, 11, pp.1231-1236.
- 12 Xu, X. F., "Phase explosion and its time lag in nanosecond laser ablation", Applied Surface Science, 2002, 197, pp.61-66.

- 13 Xu, X. F., and Song, K. H. "Phase change phenomena during high power laser-materials interaction", *Materials Science and Engineering: A - Structural Materials Properties Microstructure And Processing*, 2000, 292, 2, pp.162-168.
- 14 Xu, X. F., and Song, K. H. "Interface kinetics during pulsed laser ablation", *Applied Physics: A - Materials Science & Processing*, 1999, 69, 7, pp. S869-S873
- 15 Prasad, M., Conforti, P. F., and Garrison, B. J. "Coupled molecular dynamics-Monte Carlo model to study the role of chemical processes during laser ablation of polymeric materials", *Journal of Chemical Physics*, 2007, 127, 8.
- 16 Cooper, J. B., Julian, B., Morrison, H., Song, P., Albin, S., and Zhen, J. L. "Surface characterization of pulsed UV-laser modified polyamide films", *Thin Solid Films*, 1997, 303, 1-2, pp.180-190.
- 17 Kelly, R., and Miotello, A. "On the role of thermal processes in sputtering and composition changes due to ions or laser pulses", *Nuclear Instruments & Methods In Physics Research Section B: Beam Interactions With Materials And Atoms*, 1998, 141, 1-4, pp.49-60.
- 18 Lee, S. K., Chang, W. S., and Na S. J. "Numerical and experimental study on the thermal damage of thin Cr films induced by excimer laser irradiation", *Journal of Applied Physics*, 1999, 86, 8, pp.4282-4289.
- 19 G. W. Yang, "Laser ablation in liquids: Applications in the synthesis of nanocrystals", *Progress in Materials Science*, 2006, **52**, 4, pp.648-698.
- 20 Fabbro, R., Peyre, P., Berthe, L., and Scherpereel, X. L. "Physics and applications of laser-shock processing", *Journal of Laser Applications*, 1998, 10, 6, pp.265-269.
- 21 Zhu, S., Lu, Y. F., Hong, M. H., Chen, X. Y., "Laser ablation of solid substrates in water and ambient air", *Journal of Applied Physics*, 2001, 89, 3, pp.2400-2403.
- 22 H. Kawamoto. "The history of liquid crystal displays", *Proceedings of the IEEE*, 2002 **90**, 4, pp.460-500
- 23 Elaboudi, I., Lazare, S., Belin, C., Talaga, D., and Labrugere C. "Underwater excimer laser ablation of polymers", *Applied Physics A*, 2008, 92, 4, pp.743-748.

- 24 Elaboudi, I., Lazare, S., Belin, C., Talaga, D., and Labrugere C. "From polymer films to organic nanoparticles suspensions by means of excimer laser ablation in water", *Applied Physics A*, 2008, **93**, 4, pp.827-831.
- 25 Elaboudi, I., Lazare, S., Belin, C., Talaga, D., and Labrugere C. "Organic nanoparticles suspensions preparation by underwater excimer laser ablation of polycarbonate", *Applied Surface Science*, 2007, **253**, 13, pp.7835-7839.
- 26 Parvin, P., Jaleh, B., Sheikh, N., and Amiri, N. "Surface effect of KrF laser exposure on ECE of alpha particle tracks in polycarbonate polymer", *Radiation Measurements*, 2005, **40**, 2-6, pp.775-779.
- 27 Zangeneh, H, R., Parvin, P., Zamanipour, Z., Jaleh, B., Jelvani, S., Taheri, M., "Submicron structural alteration of polycarbonate surface due to ArF laser irradiation at high doses and the subsequent electro-chemical etching treatment", *Radiation Effects and Defects in Solids*, 2008, **163**, 11, pp.863-171.

List of Figures

Figure 1 - The result of repeatable errors in macroscopic beam shape over a number of pulses.

Figure 2 - Comparison of vapour plumes in air (left) and liquid immersion (right) and the impedance of the the liquid to the plume expansion.

Figure 3 - A measurement taken using a beam profiler from a 248 nm masked beam.

Figure 4 - Schematic of liquid immersion rig.

Figure 5 - Comparison between feature machined (a) out of focus in ambient air and (b) out of focus under thin film laminar flow water immersion.

Figure 6 - Ablation threshold plot for ambient air, normal liquid immersion and anomalous immersion.

Figure 7 - Plot of ablation rate in ambient air and under DI water liquid immersion.

Figure 8 – Graph plotting out of focus laser beam pulse energy against thickness of liquid medium traversed.

List of Tables

Table 1: Values for beam energy requested from the laser at source and actual spot energies after passing through the mask and final optic used for threshold measurement.

Table 2: Values taken listing the number of pulses used and the corresponding beam energy after the final optic of the system for ambient air and immersion machining.

FIGURE 1

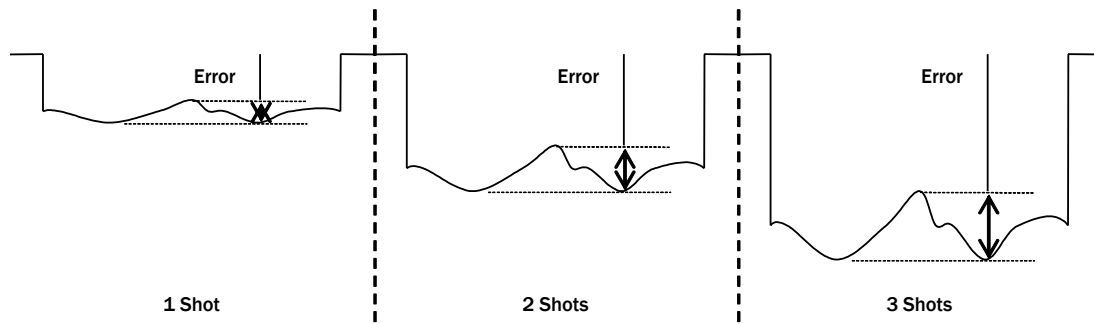


FIGURE 2

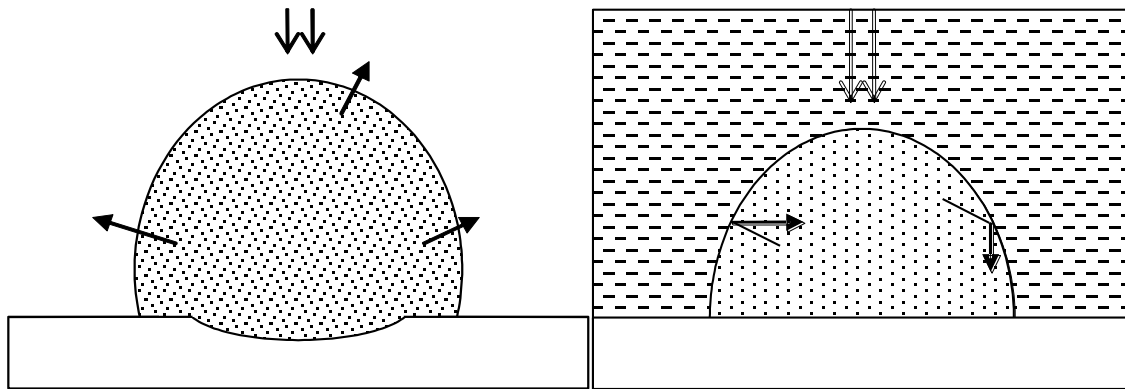


FIGURE 3

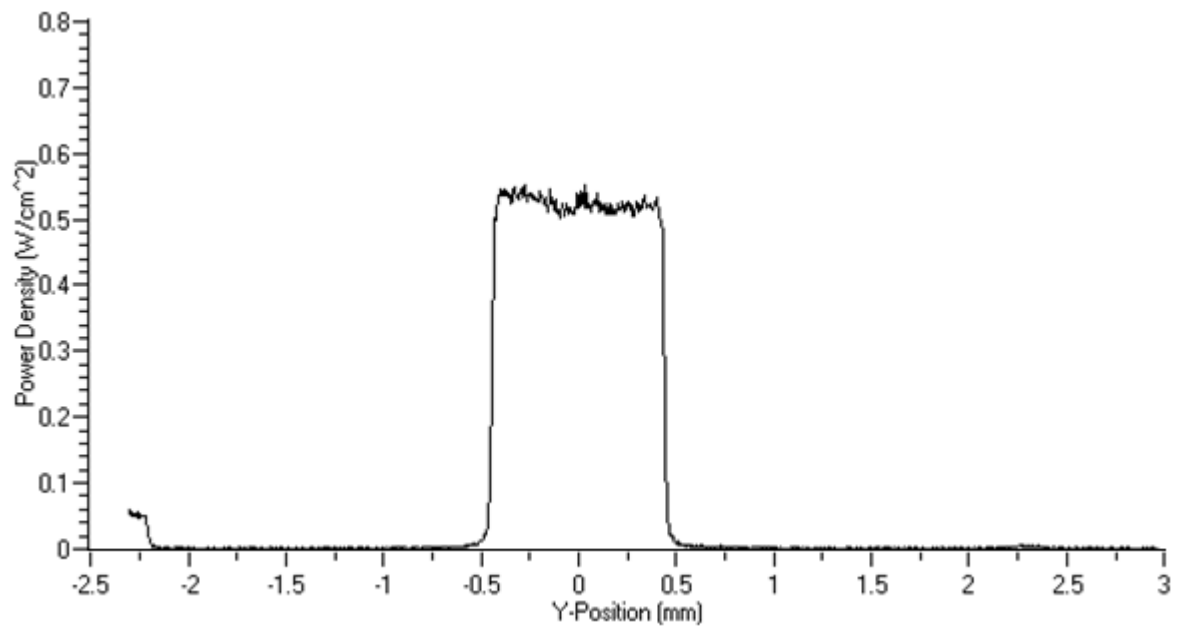


FIGURE 4

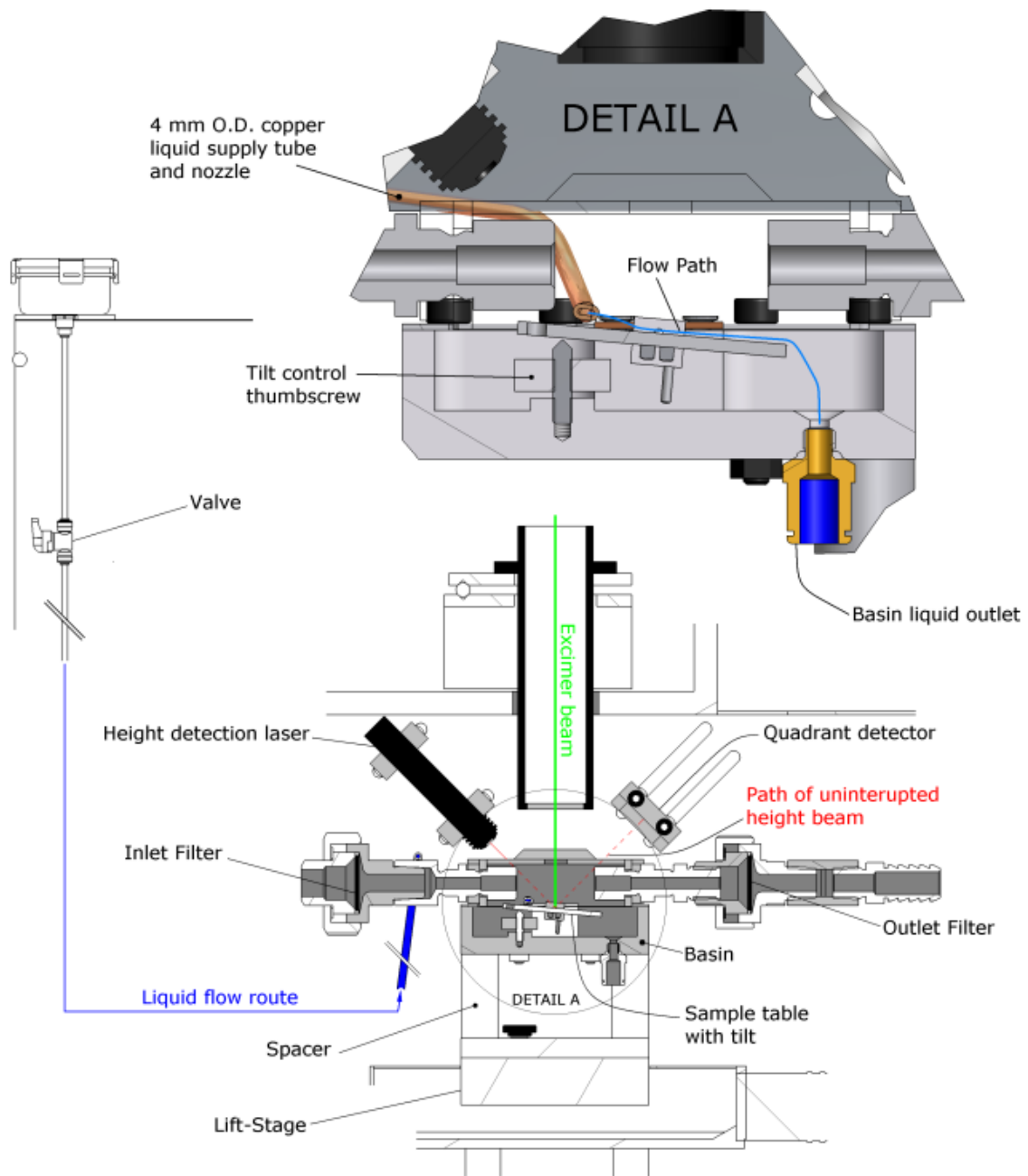


FIGURE 5

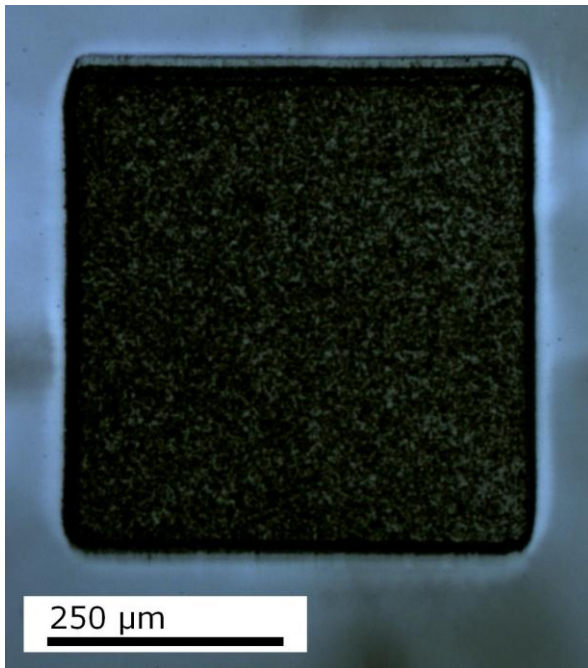


FIGURE 6

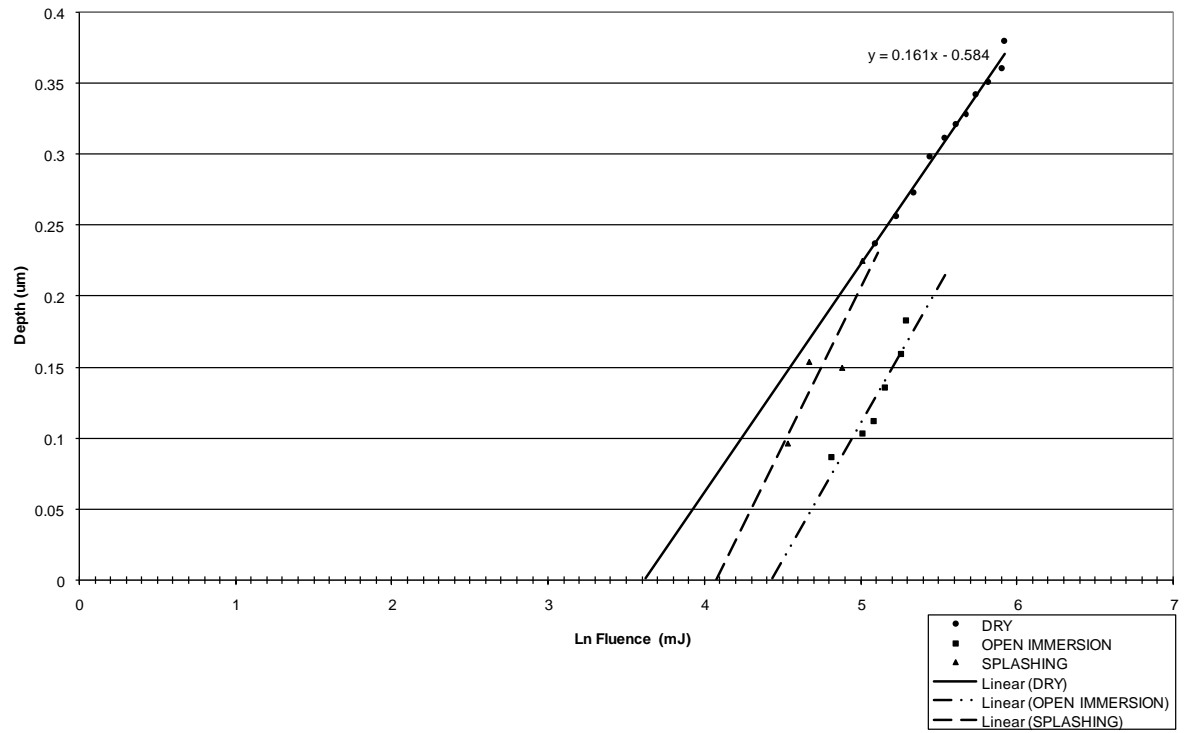


FIGURE 7

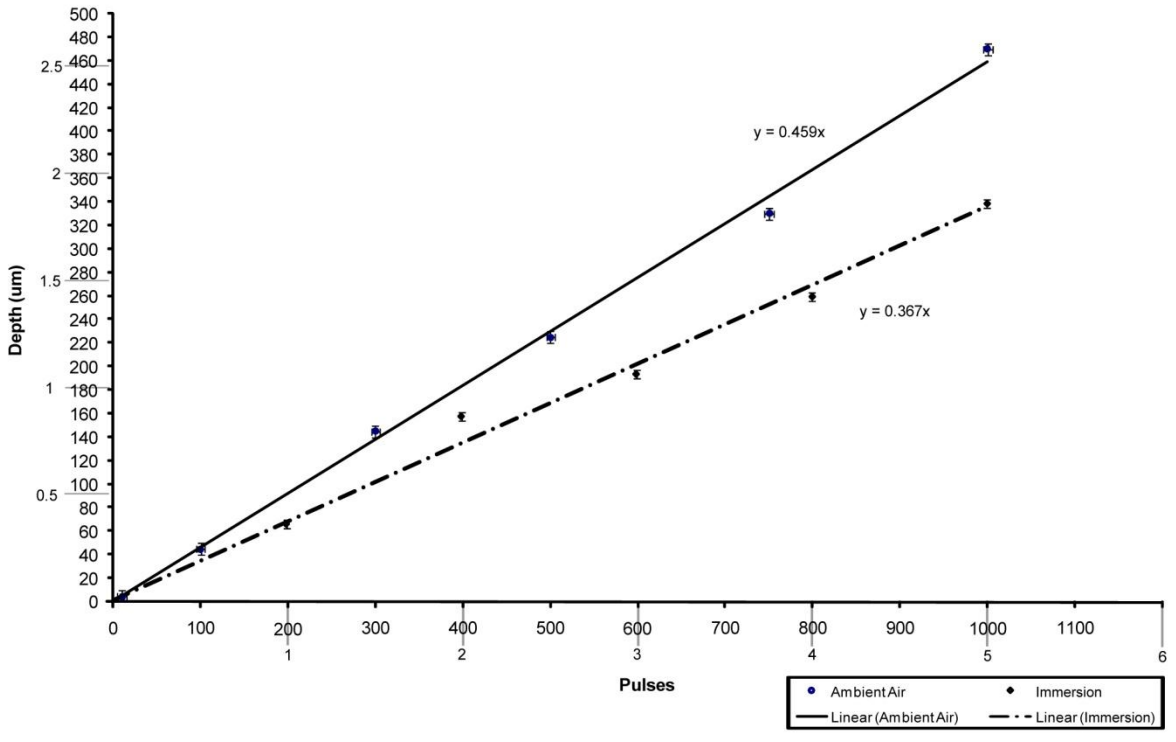


FIGURE 8

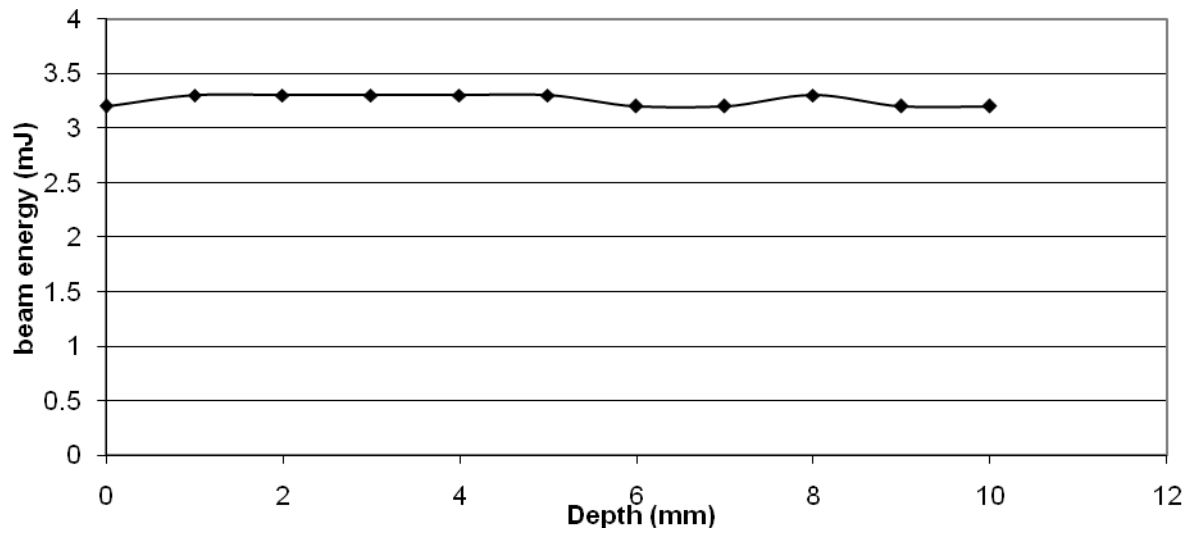


TABLE 1

A	B	C
Laser energy (mJ)	Ambient Spot Energy (mJ)	Immersion Spot Energy (mJ)
300	6.45	
280	6.15	4.35
260	5.8	4.2
240	5.35	3.8
220	5.05	3.55
200	4.7	3.3
180	4.4	3.3
160	4	2.9
140	3.6	2.7
120	3.2	2.35
100	2.8	2.05

TABLE 2

A	B	C	D
Number of Dry Pulses	Ambient Spot Energy (mJ)	Number of immersion Pulses	Immersion Spot Energy (mJ)
10	6.5	1	7
100	6.5	2	6.55
300	7	3	6.7
500	6.8	4	6.35
750	6.75	5	6.45
1000	6.7	6	
1500	6.45		
2250	6.6		
3000	6.6		
4000	5.9		